Sascha Hilgenfeldt
Faculty of Applied Physics, University of Twente
Postbus 217, 7500 AE Enschede
sascha@tn.utwente.nl

Overzichtsartikel

Bubble geometry

Droge schuim in rust evolueert naar een toestand waar de totale oppervlakte van de schuimbellen is geminimaliseerd. Dit proces veroorzaakt groei bij enkele luchtbellen en inkrimping bij andere. Vijftig jaar geleden toonde John von Neumann aan dat in tweedimensionaal schuim de groeiratio enkel afhangt van het aantal zijden van de polygonale schuimbel. Sascha Hilgenfeldt laat zien dat een goede indicator van de groeiratio in drie dimensies het aantal zijvlakken van de polyhedrale schuimbel is. De analytische theorie en de numerieke simulaties komen bovendien goed overeen.

Foams are of interest to a large and very diverse community of scientists, for a variety of different reasons. Engineers use foams in many applications of great economical impact, from firefighting to mineral processing and from oil recovery to the food sciences (Note that many of the processed foods we eat are foams, such as bread, cake, ice cream, chocolate bars, beer and soda foams, etc.). Overviews can be found in books such as Bikerman's [1] and Prud'homme's [2]. In relation to recent gruesome events, it is worth noting that special detergent foams are the means of choice for the decontamination of areas exposed to biological weapons. Foams are also a prime example of soft condensed matter with viscoelastic properties and complex flow behavior (rheology) similar to emulsions [3–4]. The flow through liquid foams has been the subject of extensive studies by physicists (see [2, 5–7] for more information). As stable foams demand a good surface-active agent (surfactant), surface chemistry is another field that widely uses foams and single surfactant films [8–9]. And finally, mathematicians have been fascinated by the shape and structure of soap films and bubbles for centuries, largely because their tendency to minimize surface area makes them experimental models for minimal surfaces and tilings of space [10–11].

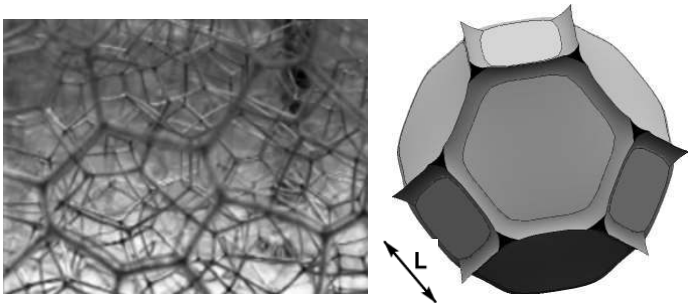

Figure 1 a (left): A view of a dry aqeuous foam, from [12]; the bubbles are polyhedral. b (right): Geometry of a single foam polyhedron with typical edge length L. Almost all liquid is concentrated in the channels. This particular bubble is a simulation of a wet Kelvin cell (cf. figure 10 for the ideally dry version).

Modern foam research starts with the Belgian mathematician and scientist Joseph Antoine Ferdinand Plateau, who in the 1870s formulated the basic rules of foam geometry that bear his name today and will be discussed later in this article. Incredibly, Plateau did most of this groundbreaking research when he was almost completely blind, with his assistants carrying out the experimental procedures.

The geometrical properties of foam structures in turn have direct bearing on other cellular matter. Instead of delineating the structure of a dry foam, figure 1a could as well be a faithful representation of grains in a polycrystalline metal or cells in the epidermis of a plant. Nor is this relation only superficial: the problem of filling space with minimal expenditure of energy (i.e., surface area) is common to all of these structures, so that their geometrical similarity has functional reasons. How to describe the cellular structure and its potentially universal characteristics is, however, not at all clear today. The recent work described here has elucidated some aspects of the evolution of this structure, and may be instrumental to its eventual detailed description.

By way of introduction, let us take a closer look at the geometry of one bubble forming part of a liquid foam. Figure 1 shows that, for low liquid content, the bubbles are not at all spherical, but they are polyhedra with slightly curved edges and faces. Physically, the faces are two parallel surfactant layers between which a thin film of liquid is enclosed. That amount of liquid is, however, negligible compared to the liquid residing in the channel-like structures that delineate the edges of the polyhedron (figure 1). The resistance to liquid flow is therefore lowest in these channels (also known as Plateau borders), and this is where *foam drainage* occurs. While drainage is an intensely discussed topic in its own right at the moment [7, 13–16], we will disregard it here, assuming that the foam is so dry that the channels degenerate into line edges,

and we can treat the bubble as an ideal polyhedron with no liquid present, but the complete edge and face structure intact (cf. figure 7 below). In other words: both the films and the edges are now assumed of vanishing thickness, making them two- and one-dimensional structures, respectively. The typical length L of an edge serves as a measure of linear bubble size.

Any polyhedron (whose closed surface is topologically equivalent to that of a sphere) in 3-D space has to obey Euler's theorem,

$$U - E + F = 2\,,$$

where U, E, and F are, respectively, the number of vertices, edges, and faces of the polyhedron. For dry foam bubbles, the polyhedral geometry is further restricted: *Plateau's rules* are valid, which require faces to meet in threes under tangential angles of $2\pi/3$, and edges to meet in fours under tetrahedral angles (figure 2). Empirically formulated in 1873 by Plateau, it took more than 100 years to prove [17] that these are the only stable conformations of polyhedra in a foam of uniform surface tension. The coordination numbers of Plateau's laws enforce $2E = 3U$, and therefore

$$E = 3F - 6 \qquad (1)$$

follows for any foam polyhedron. In other words, for polyhedra in a foam either of the three quantities U, E, F determines the other two. We will make use of this later.

Coarsening

Foam drainage is not the only process of dynamical evolution in a liquid foam. Because the films are thin, gas can readily diffuse through them from one bubble to another. This leads to increased volume of some bubbles that grow at the expense of others. Eventually, some of the bubbles shrink to zero volume (disappear), and — if we assume that the total foam volume is conserved — the average bubble size (or edge length L) increases over time. This process is called *coarsening* and is a direct consequence of the metastability of a foam: as the creation of a surface area element dA costs surface energy $dE_s = \gamma dA$ (with the surface tension γ), a foam with its many interfaces is in an energetically undesirable state. Ideally, all the bubbles would merge into a single gas volume, which is the actual stable state.

Well-separated grains

The same process is at work wherever phase separation has generated grains, droplets, or bubbles of a dispersed phase in a continuous medium in which the solubility of the dispersed phase is nonzero, so that diffusive exchange of molecules between the 'islands' is possible. For isolated grains of roughly spherical size (figure 3), this process has been known for a long time as *Ostwald ripening*, and it is theoretically well understood (see e.g. [18]). If the limiting time step is diffusion (and not the kinetics of the actual adsorption to a grain), the field of dispersed-phase concentration around a grain decreases as $1/(\text{distance})^2$ [19], and the average radius of grains grows as $\langle R_g \rangle \propto t^{1/3}$. The situation is different for kinetically limited exchange of material: the concentration field can then be assumed constant with distance, and the growth accelerates to $\langle R_g \rangle \propto t^{1/2}$ [18–19]. It should be stressed that the prefactors of these growth laws are also known. Likewise, analytical results were derived for denser systems of still-isolated, spherical grains [20].

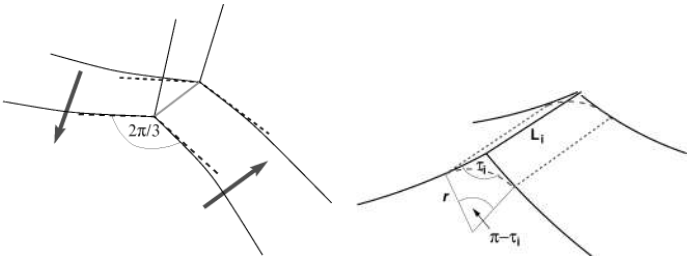

Figure 2 (a) An edge of a foam polyhedron is always a junction of three faces. Even though the faces can be curved in various ways, stability of the configuration demands that the tangential angle at the edge must be $2\pi/3$ (Plateau's rule). The figure also illustrates the direction of coarsening, which depends on the face curvature: gas is lost through convex faces and gained through concave faces (arrows). (b) Mean curvature is concentrated at an edge with tangential angle τ_i. As the radius r goes to zero, the mean curvature integral over the cylindrical section (dashed) reduces to $(\pi - \tau_i)L_i/2$.

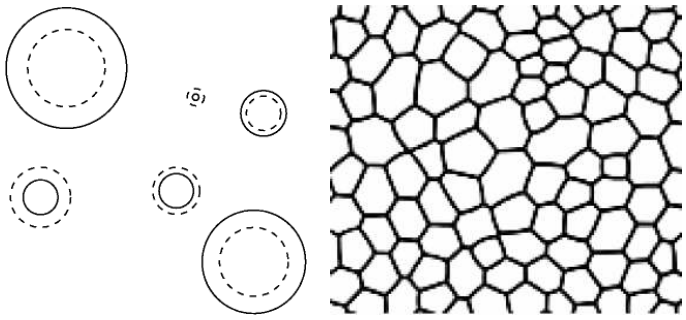

Figure 3 (a) Sketch of Ostwald ripening in 2-D: small grains with higher curvature shrink and dissolve, feeding the growth of larger grains (solid outlines indicate a later time than dashed outlines). (b) A two-dimensional dry foam or other cellular material where the dispersed phase has almost completely invaded the continuous phase. The grains are now polygonal instead of round.

The question here arises if such a coarsening material has a universal distribution of grain sizes: if one rescaled figure 3 by the average grain size $\langle R_g \rangle(t)$, would it look — statistically — the same for all times t? Lifshitz and Slyozov [21] and Wagner [22] first showed that the size distribution in this system indeed tends towards *statistical self-similarity*. The formalism, now known as LSW theory, is very valuable in particular for metallurgy, where grains in polycrystalline metal melts grow due to Ostwald ripening.

Cellular structures

Given a sufficient total amount of dispersed-phase material coming out of solution from the continuous phase, the grains will grow until they touch each other, and must then lose their sphericity. When almost all the dispersed phase has been expelled, what remains is a cellular structure (figure 3) that is equivalent to a dry foam. But for the reasons outlined above, this is not the end point of evolution, as the total interfacial area can be reduced further by the growth of some polyhedral grains at the expense of others. This stage of Ostwald ripening is not well-understood at all, because the complex geometry of the emerging cellular structure begins to play a huge role for the rates of the coarsening. The power law of growth is still easily derived: as the distance between grains is now negligible compared to the grain size, even a diffusion-controlled process now yields a linear-scale growth of $L \propto t^{1/2}$. Then, $L\dot{L}$ must be a constant (where $\dot{L} = dL/dt$). Dimensional analysis shows it to be a diffusion coefficient. However, the prefactor also contains information about the structure of the foam which can not be normalized out as a mere material

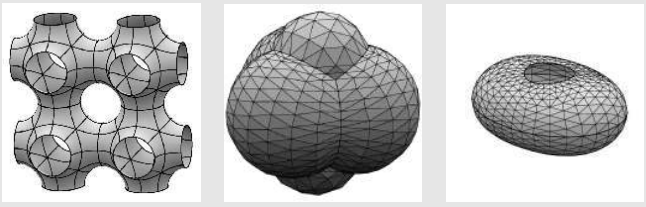

Figure 4 From left to right, Schwarz P surface, cluster of five bubbles, shape of a droplet on a spinning rod. Images available under [32].

The Surface Evolver

The Surface Evolver is a software developed by Ken Brakke at University of Minnesota since the early 1990s. It is specifically designed to find minimal energy configurations of interfaces under almost arbitrary constraints, and to find the evolution path towards those optimal states. The Evolver can handle interfaces of arbitrary topology and almost arbitrary dimension. Interactive modifications of the computed surface are also possible. The software has been used to study many problems in mathematics and the physical sciences, such as minimal surfaces, sphere eversion, or lipid vesicle shapes. See figures 1, 4, 7, and 10 in this article for a few examples.

Maybe the best feature of the Surface Evolver is that it is freely available to everyone, for a variety of computer platforms. Downloads, documentation, and more information can be found in [32].

parameter. More precisely, we can write

$$\dot{L}L = D^*_{\text{eff}} F(\text{geometry}) \,, \tag{2}$$

where the effective diffusion coefficient $D^*_{\text{eff}} \equiv D_{\text{f}} \text{He} \gamma v_m / d_{\text{f}}$ incorporates all the material parameters, i.e., film diffusion coefficient D_{f}, solubility constant from Henry's law He, surface tension γ, molar volume v_m and film width d_{f}. The dimensionless function F depends only on the bubble geometry, i.e., the angles and edge lengths of the polyhedron, along with the curvature of its faces.

It is possible to be more specific about the function F by revisiting the physical force that drives the gas exchange through the films. The biased diffusion is the consequence of a *pressure difference* between the two bubbles separated by a particular face. By the Young–Laplace law, this pressure difference Δp is directly connected to the mean curvature H of the film,

$$\Delta p = 4\gamma H = 2\gamma \left(r_1^{-1} + r_2^{-1} \right) \,,$$

where $r_{1,2}$ are the principle radii of curvature of the polyhedral face and $H = (r_1^{-1} + r_2^{-1})/2$ must be constant over the face (otherwise its shape would change). The additional factor of 2 comes from the existence of *two* parallel faces enclosing the thin film between neighboring bubbles.

We can now conclude that $F \propto \int_{\text{faces}} H dA$, where the integral is evaluated over all interfaces of the bubble. Figure 2 illustrates this dependence of pressure difference, and therefore gas flow, on the curvature of the interface: if curved outward, gas is lost through the face, if curved inward, gas is gained through it. Still, with all the different possible shapes of bubbles this seems an impractical ansatz to determine the coarsening rates of a foam as a whole, or deduce self-similar size distributions. Indeed, the grain volume distribution of a coarsened three-dimensional cellular material is still unknown. However, great progress was made for the *two-dimensional* analog.

Von Neumann's law (2-D)

A two-dimensional dry foam can be envisaged as a single layer of bubbles confined between parallel glass plates whose distance is smaller than the bubble size. Then, as seen from above, the bubbles are polygons with curved edges. They are still separated by (one-dimensional) films and will still exchange gas and undergo coarsening. In 1952, John von Neumann, while attending a lecture by C. S. Smith on metal grains and coarsening, noticed that for this case the mean curvature of the interface was very easy to determine. For every curved edge i of the polygon, $H = 1/R_i$, with a fixed radius of curvature R_i (see figure 5), the rate of growth of

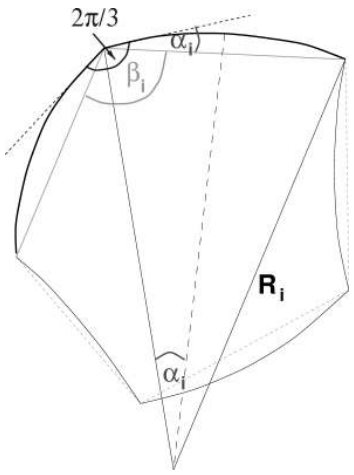

Figure 5 Sketch of a polygonal bubble with curved edges, illustrating the proof of von Neumann's 2-D law of bubble coarsening. Details are given in the text.

the area of a polygon $\dot{a}$ is then proportional to $\int_s H ds$. The integration runs over all n edges indexed with i, whose length is given by $\alpha_i R_i$ (the angles α_i are defined in figure 5). So we obtain

$$\dot{a} \propto \int_s H ds = \sum_i \frac{1}{R_i} \alpha_i R_i = \sum_i \alpha_i \,.$$

The sum over the angles α_i is easily obtained, as α_i is one-half of the difference between the tangential angle under which the edges meet in a vertex (this tangential angle is $2\pi/3$, by Plateau's law) and the angle β_i under which the edges would meet if they were straight (see figure 5). From elementary geometry, $\sum_i \beta_i = (n-2)\pi$, and therefore $\sum_i \alpha_i = -\frac{\pi}{6}(n-6)$.

Thus, von Neumann arrived at the remarkable result that the growth or shrinkage rate of a 2-D bubble in a dry foam does not depend on its shape or size, but the only geometrical quantity that matters is the number of edges n. Absorbing all other (material) parameters in an effective diffusion coefficent D_2, *von Neumann's law* is

$$\dot{a} = D_2 (n - n_0) \,, \tag{3}$$

which is an exact formula for every individual bubble, and the edge number of neutral growth is exactly $n_0 = 6$. Bubbles with fewer edges shrink, those with more edges grow. Note that the

population of bubbles with n edges may stay constant nevertheless: For instance, when a small triangular bubble disappears (shrinks to a point), its three neighbors all lose one edge, so that even a bubble that starts out growing may be 'downgraded' to a shrinking bubble, replenishing the small-n population.

A conjecture about 3-D coarsening

Von Neumann published this result as a written discussion to C. S. Smith's talk [23]. Smith was very excited about the result and hoped for a generalization to the case of three-dimensional, polyhedral foams [23], where the edge number n would be replaced by the number of faces F. Unfortunately, this problem is not as benign. Just by constructing counterexamples, it is easy to verify that a direct analog of (3) in three dimensions does not exist: it is possible to have valid foam polyhedra with the same F, but different integral mean curvatures, and therefore different growth rates. While there is no 3-D von Neumann law in the strict sense, another question was asked soon after von Neumann's discovery: is there an analog to (3) which is valid for the *average* bubble with F faces? Upon averaging over all bubble geometries with the same F using the average $\langle\cdot\rangle_F$, a *statistical* growth law looks like this:

$$V_F^{-1/3}\dot{V}_F = D_{\mathit{eff}}G(F) \equiv -D_{\mathit{eff}}V_F^{-1/3}\left\langle \int_{\text{faces}} H dA \right\rangle_F , \qquad (4)$$

where $V_F = \langle V\rangle_F$ is the averaged volume of all bubbles with F faces in the foam, and D_{eff} another effective diffusion coefficient. Note that the combination $\dot{V}_F V_F^{-1/3}$ is, up to a constant, just the term $\dot{L}L$ from (2). Lumping all material parameters into D_{eff}, the problem is tantamount to determining the dimensionless growth function $G(F)$.

Many arguments and numerical simulations were introduced [24–27] to suggest that a linear growth law of the form $G \propto (F - F_0)$ should exist, i.e., again a linear dependence of growth rate on F, with a face number F_0 for neutral growth. We will show here that this conjecture turns out to be false.

Experiments and simulations

Attempts at an experimental verification of this conjecture met with great difficulties: While the existence of a neutral growth face number F_0 could be verified [28] (it was found that F_0 was between 13 and 14), the experiments were confined to values $F \approx F_0$, and so could not verify the functional form of the geometry dependence. Also, the statistics of the measurements only comprise a handful of bubbles [29–30].

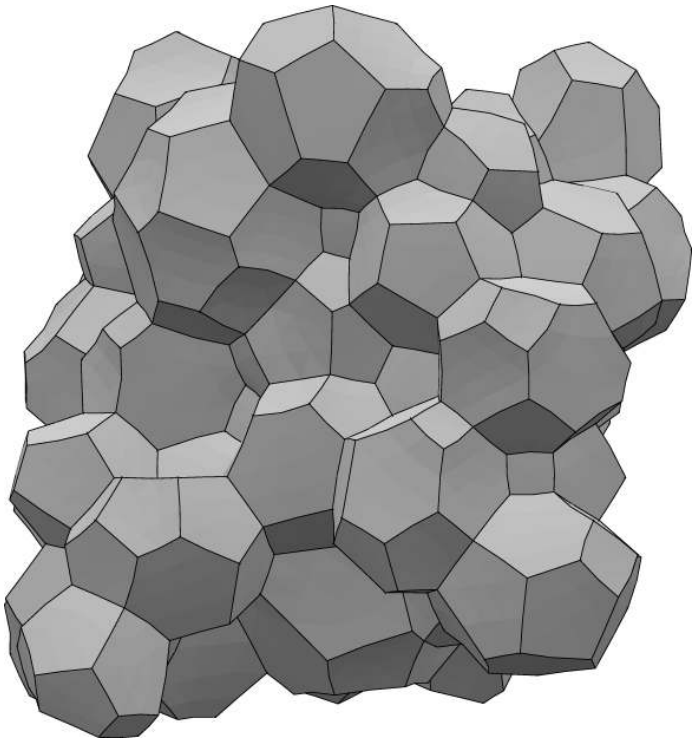

Figure 7 Random polydisperse foam generated with the help of the Surface Evolver program. This example simulation comprises 64 bubbles, while up to 1000 cells per run have been calculated. (Figure courtesy of Andy Kraynik)

The main problem in these experiments is the long coarsening time scale that does not allow for long-time data of the coarsening dynamics. Another possibility to derive growth and shrinkage rates is to determine the curvature of interfaces between bubbles directly, which (see above) is proportional to the rate of gas exchange. Even static foams can thus give information about coarsening rates. The curvature of the tenuous films is very hard to visualize in experiment, but numerical simulations can determine it easily using the Surface Evolver, a program specifically designed to minimize surface areas under geometrical constraints [31]. Kraynik [33] has conducted Surface Evolver simulations of random 3-D foams with up to 1000 bubbles, either monodisperse or polydisperse in volume (see figure 7 for a smaller example). While no actual gas diffusion is simulated, the interface curvatures supply the growth data for $G(F)$ shown as circles in figure 6.

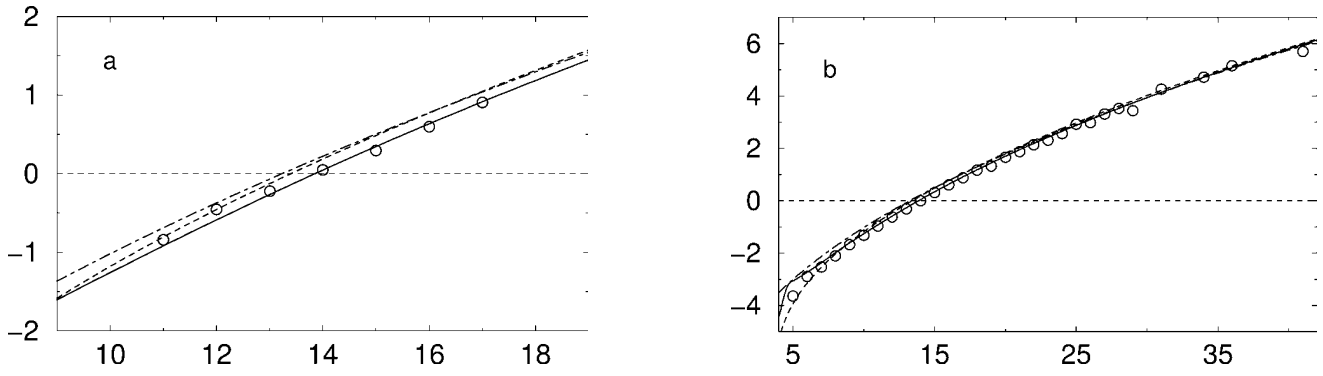

Figure 6 Growth function $G(F)$ of a random foam. Circles show simulations with the Surface Evolver, for (left) 512 monodisperse and (right) 512 strongly polydisperse bubbles. Dashed and dot-dashed lines result from the analytical expressions (11) and (12). The solid line is from a refined theory [34] incorporating the disorder of the simulated foam, characterized by $\sigma_\eta = 0.73$ (see text).

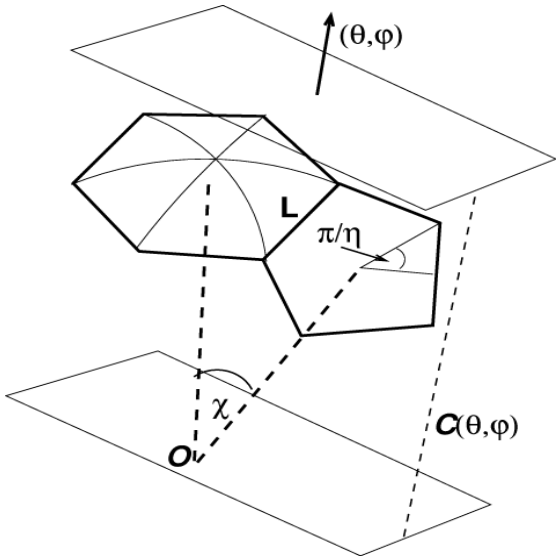

Figure 8 Sketch of two adjacent polygonal faces on a polyhedral foam bubble with centroid O. Indicated are the angle between face normals χ, edge length L, and planar angle π/η for a regular face with η edges. The two planes illustrate the definition of the caliper radius $C(\theta,\varphi)$ (see text).

Note the much wider range of F accessible in polydisperse foams. The statistical error of these averages is on the order of the symbol size for most data points, while the spread of growth rates between individual bubbles with the same F is larger (typically ± 0.2). The simulations show that indeed bubbles with large F tend to grow and those with small F tend to shrink, but they also give evidence that $G(F)$ might *not* be linear in F as conjectured. Is it possible to find an analytical approximation to the actual growth function, i.e., can we really find an analog to what von Neumann did 50 years ago?

Von Neumann's law in three dimensions

To determine which bubbles in a 3-D foam grow and which ones shrink, we have to understand how the integral mean curvature over the bubble faces depends on its other geometrical properties. Fortunately, there are classical studies on this subject by Hermann Minkowski. In 1903 [35], he related mean curvature over the surface of a convex body to a quantity we call the *caliper radius* $C(\theta,\phi)$ here, whose definition is illustrated in figure 8. Choosing a coordinate origin O in, e.g., the center of mass of the body, we draw a plane through O perpendicular to the spatial direction (θ,ϕ). A second, parallel plane is then moved as far away as possible while still touching the body. The distance between the planes (the 'extent' of the body in the direction (θ,ϕ)) is the caliper radius $C(\theta,\phi)$. Minkowski proved that

$$\int_{4\pi} C(\theta,\varphi)d\omega = \int_{S_K} HdA \qquad (5)$$

for any convex body K, where the integrals are over all solid angles ($d\omega = \sin\theta d\theta d\varphi$) and the total surface area S_K of K, respectively. Following the proof of this theorem as outlined e.g. in [36], one can verify that it remains valid for a body that is not convex, but piecewise convex or concave (such as a faceted foam polyhedron), if the definition of $C(\theta,\phi)$ is suitably generalized. Note also that the integral mean curvature over the surface of a faceted body consists of two contributions: the mean curvature of the faces, and the concentrated mean curvature in the edges, which depends on the tangential angle under which the faces meet in the edge. Figure 2 illustrates that this curvature contribution is simply

$$\int_{\text{edges}} HdA = \sum_{i=1}^{E} \frac{1}{2}(\pi - \tau_i)L_i\,, \qquad (6)$$

where τ_i is the tangential angle and L_i the length of edge i ($i = 1,\ldots,E$).

We will now apply (5) to two different bodies: a foam polyhedron K, whose edges are *curved*, and its *skeleton polyhedron* K_0, i.e., a polyhedron with the same vertex positions where the faces have been replaced by (piecewise) *flat* faces. In complete analogy to von Neumann's 2-D argument, we can then evaluate the difference between the edge curvatures (6) of K and K_0: as $\tau_i = 2\pi/3$ by Plateaus law for foam polyhedra, the edge curvature is just $\frac{\pi}{6}\sum_i L_i$ for K, while it is $\sum_i \frac{1}{2}\chi_i L_i$ for K_0, where $\chi_i = \pi - \tau_i$ are the angles between adjacent face normals (figure 8). Now we can write Minkowski's theorem as

$$\int_{4\pi} C(\theta,\varphi)d\omega = \int_{\text{faces}} HdA + \sum_{i=1}^{E} \frac{\pi}{6}L_i \qquad (7)$$

for K, and

$$\int_{4\pi} C_0(\theta,\varphi)d\omega = \int_{S_{K_0}} HdA = \sum_{i=1}^{E} \frac{1}{2}\chi_i L_i \qquad (8)$$

for K_0, as the integral over the flat faces vanishes. The importance of Minkowski's theorem is that the left-hand sides of (7) and (8) can be directly evaluated by expanding C around C_0 in a series over the small parameter $\epsilon = L/R$, where L is a typical edge length and R a typical radius of curvature of the bubble. By inspection of bubbles in real foams, we know that $\epsilon \ll 1$. The result of this computation gives

$$\int_{4\pi} C(\theta,\varphi)d\omega - \int_{4\pi} C_0(\theta,\varphi)d\omega = L\,O(\epsilon^3)\,,$$

i.e., the difference between the left hand sides of (7) and (8) is of third order. Consequently, by setting the right-hand sides equal to each other, we find an expression for the integral curvature over the faces, which is precisely the quantity that we need to evaluate the growth rate (cf. (4)). We obtain

$$\int_{\text{faces}} HdA = \sum_{i=1}^{E} \frac{1}{2}\left(\chi_i - \frac{\pi}{3}\right)L_i\,, \qquad (9)$$

valid to order ϵ^2. This formula tells us the growth rate for every individual bubble, but it also shows that we need much more information about a 3-D polyhedron than about a 2-D polygon to evaluate it: while the edge number E is directly given by F (see (1)), all the angles and edge lengths have to be known. To obtain a formula such as (4), we have to average over all configurations.

This averaging seems like a daunting task, and so let us try to start with the most simplistic of assumptions, namely, that all bubbles of face number F have the same geometry, and that they are maximally symmetric and isotropic, i.e., all faces have the same number of edges and all edge lengths are the same. Note that for a given F, these conditions do not prescribe an actually existing bubble; it is easy to see that each of the faces must have $\eta_F = 6 - 12/F$ edges, which is a *fractional* number for all F but 4 (tetrahedron), 6 (cube), and 12 (pentagonal dodecahedron). As we are looking for statistically averaged formulas, we will go along

with this, interpreting the idealized polyhedra as reasonable interpolations.

The idealized F-faced bubbles have equal face normal angles χ_F (figure 8), which are found to be

$$\chi_F = 2\arctan[(4\sin^2(\pi/\eta_F) - 1)^{1/2}]\,. \qquad (10)$$

Here, we can already determine the value of F_0. A neutrally growing bubble must, by (9), have $\chi_F = \pi/3$, so that $F_0 \equiv F_0^* = 12/(6 - \pi/\arcsin\sqrt{1/3}) = 13.397\ldots$, a well-known value conjectured to be the average face number in a minimal-area foam with equal pressure bubbles [11, 37]. This number also compares well with the available experimental evidence [28, 30] and the numerical simulations of figure 6.

Encouraged, we now go on to compute $G(F)$, inserting χ_F for χ_i in (9) and normalizing the result by $V_F^{-1/3}$. For the latter, the volume V_F is assumed equal to the volume of the skeleton polyhedron (the volume contributions due to the curved interfaces are neglected). Thus, we obtain [34]

$$G(F) = \frac{3\left[(F-2)\tan\frac{\pi}{\eta_F}\right]^{2/3}\tan^{1/3}\left(\frac{\chi_F}{2}\right)}{2^{1/3}}\left(\frac{\pi}{3} - \chi_F\right). \qquad (11)$$

Together with (10) and the definition of η_F, this is a completely parameter-free, analytical expression for G, which compares extremely well with the numerical simulations for both monodisperse and polydisperse foams (figure 6). The simulations — which themselves are also parameter-free — obtain $F_0 \approx 13.82$ for the monodisperse and $F_0 \approx 14.00$ for the polydisperse case, but more striking is the excellent agreement over the whole range of F, even in the polydisperse case. Note that the theory presented here does not contain any correlation between bubble size and face number, even though there is a strong correlation in real foams (smaller bubbles have smaller F). Therefore, the predictions from (11) are the same for both simulations.

The success of the simplistic picture of equal, maximally symmetric bubbles shows that the average over the shapes of foam-bubbles in a random foam must lie very close to the most compact, least distorted shape possible, so that the characterization by face number alone is a very good indication of the growth or shrinkage rate of the bubbles.

If only evaluated in the vicinity of F_0, Eq. (11) necessarily resembles a linear function, but an expansion for large F shows that its asymptote is

$$G(F \gg 1) = \frac{\pi^{7/6}}{2^{1/6}3^{5/12}}F^{1/2} - 6^{1/3}2\pi^{2/3} + O(1/F^{1/2})\,, \qquad (12)$$

a *square-root* function of F. The dot-dashed line in figure 6 shows that approximation, which works very well even for relatively small F.

One can try to improve further on this result by relaxing the condition of uniform bubble shape, introducing variations in edge number, edge length, etc. This is rather cumbersome, and the interested reader is referred to [34] for the details of the actual procedure. As a measure for disorder, we use the width σ_η of the distribution of edge numbers η, which we take to be universal for all face numbers F, centered around the idealized values η_F. The parameter σ_η does change from random foam to random foam: for Kraynik's simulations [34], we find $\sigma_\eta \approx 0.73$. Plugged into this formalism, it leads to the solid $G(F)$ curve in figure 6, which is now extremely close to the numerical result, with $F_0 \approx 13.85$, agreeing with simulation to three significant figures. The static experimental random foams from the remarkable paper by Matzke [38] have $\sigma \approx 0.59$; they would yield a slightly different growth curve, and also a slightly different F_0. Further analysis shows (figure 9) that with growing disorder parameter σ_η, F_0 departs quadratically from the idealized value F_0^*. However, realistic foams never seem to stray very far from this figure.

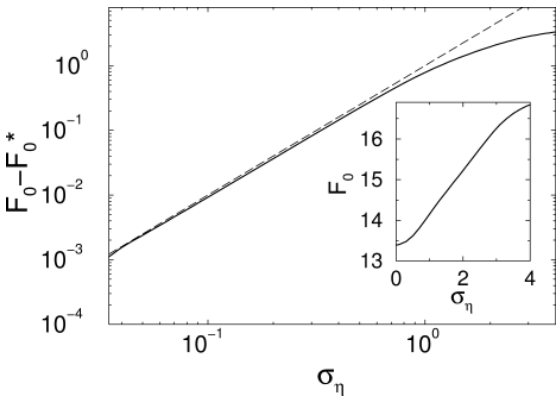

Figure 9 Solid lines: dependence of neutral growth face number F_0 on the foam disorder σ_η (width of the edge number distribution). The inset and main figure show the same curve on linear and log-log scales, respectively. The dashed line indicates a quadratic power law for small $F_0 - F_0^*$.

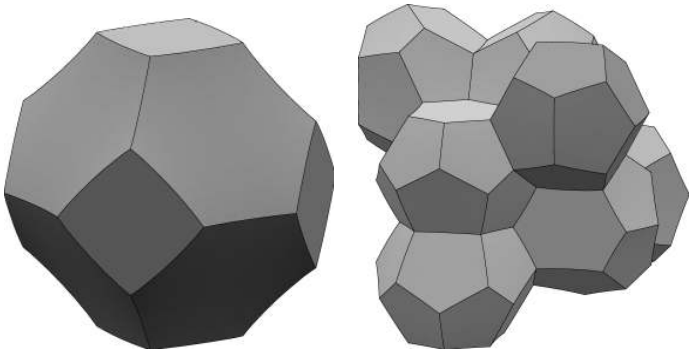

Figure 10 a (left): Kelvin's 1887 conjecture for the unit cell of the optimal tiling of space. This 14-faced cell looks much like the Wigner–Seitz cell of a bcc crystal, but its edges and faces are slightly curved. b (right): Weaire and Phelan's 1994 counterexample unit cell consisting of eight polyhedra (six 14-faced, two 12-faced). It is not known if this cell is indeed optimal.

Conclusion and outlook

We have derived a three-dimensional analog to von Neumann's law for the coarsening growth rate of bubbles in a foam. While not valid for individual bubbles, the 3-D version does a very good job capturing the behavior of averaged polyhedral bubbles with a given number of faces, and can thus be said to describe the coarsening of the whole ensemble of foam polyhedra. The analytical 3-D von Neumann's law (11) depends on the number of faces alone, and demonstrates that F is the most important parameter determining growth or shrinkage of coarsening bubbles, much like the number of edges in two dimensions. However, the growth rate does not increase linearly with the number of faces, but asymptotically as the square root.

Work is currently underway to put the 3-D von Neumann law to similar good use as the 2-D law. The latter has been instrumental to help predict the size and shape distributions in two-

dimensional cellular matter that is well-coarsened (e.g. [39–40]). As mentioned in the introduction, the properties of these functions are largely unknown for the 3-D case, with the exception of some necessary conditions they must fulfill, cf. [19]. The relatively simple form of (11), and in particular of the approximation (12), gives hope as to the existence of simple analytical predictions for the structure of 3-D foams, polycrystalline metals, living cells, and other similar materials.

It is also tempting to speculate about the impact of this work on the long-standing and still unsolved question of the optimal tiling of space, known as the Kelvin problem [11]. The problem is often posed like this: if you want to tile a 3-D space completely with objects of unit volume, what is the tiling for which the total interfacial area is minimized? Lord Kelvin conjectured a solution, namely a tetrakaidecahedron ($F = 14$, eight hexagonal, four square faces) with slightly curved faces that tiles space (figure 10). The conjecture survived for more than a century, but in 1994 Weaire and Phelan [41] found a counterexample (using the Surface Evolver), a periodic foam with a more complicated unit cell consisting of six tetrakaidecahedra (of another kind, with 12 pentagons and two hexagons) and two pentagonal dodecahedra (figure 10). This structure is also known as A15 in crystallography, where it occurs for various minerals and metal alloys [11]. The differences in surface/volume efficiency for these two structures is minute (they differ by fractions of a percent), but the Weaire–Phelan structure seems more realistic for a foam, in particular as it contains many pentagonal faces. Pentagons are abundant in real foams [38], while a foam made from Kelvin cells does not contain any of them. Not surprisingly, Kelvin cell configurations are found rarely [33] or not at all [38] in realistic foams.

The space-filling structures described in the previous paragraph are monodisperse foams, for which it can be shown that their average face number $\bar{F}$ should be equal to the neutral growth face number F_0 (cf. [42]). With the correlation between F_0 and foam disorder, this establishes a correlation between surface/volume ratio and disorder, suggesting that less disordered foams could attain lower surface/volume ratios. Maybe mathematicians could profit from this in their attempt to solve the Kelvin problem, applying a formula found because of the desire to explain the physical process of coarsening in foams, something every reader can readily observe in a glass of beer.

Acknowledgments

Many thanks to Andy Kraynik, Stephan Koehler, and Howard Stone for long-standing collaborations, and Klaus Mecke for valuable discussions.

References

1 J. J. Bikerman, *Foams* (Springer, New York, 1973).

2 *Foams: Theory, Measurements and Applications*, edited by R. K. Prud'homme and S. A. Khan (Marcel Dekker, New York, 1996).

3 A. M. Kraynik, Ann. Rev. Fluid Mech. **20**, 325 (1988).

4 T. G. Mason, J. Bibette, and D. A. Weitz, J. Colloid Interface Sci. **179**, 439 (1996).

5 G. Verbist, D. Weaire, and A. Kraynik, J. Phys. Condens. Matter **8**, 3715 (1996).

6 D. Weaire and S. Hutzler, *The Physics of Foams* (Oxford University Press, Oxford, 2000).

7 S. A. Koehler, S. Hilgenfeldt, and H. A. Stone, Langmuir **16**, 6327 (2000).

8 K. J. Mysels, K. Shinoda, and S. Frankel, *Soap Films, studies of their thinning* (Pergamon Press, London, 1959).

9 D. Exerowa and P. M. Kruglyakov, *Foam and foam films* (Elsevier, Amsterdam, 1998).

10 J. M. Sullivan, in *Foams and Emulsions*, edited by J. F. Sadoc and N. Rivier (Kluwer, Dordrecht, 1999), pp. 379–402.

11 *The Kelvin problem*, edited by D. Weaire (Taylor & Francis, London, 1996).

12 M. R. Fetterman et al., Optics Express **7**, 186 (2000).

13 S. A. Koehler, S. Hilgenfeldt, and H. A. Stone, Phys. Rev. Lett. **82**, 4232 (1999).

14 M. Durand, G. Martinoty, and D. Langevin, Phys. Rev. E **60**, R6307 (1999).

15 A. Saint-Jalmes, M. U. Vera, and D. J. Durian, Europhys. Lett. **50**, 695 (2000).

16 S. Hilgenfeldt, S. A. Koehler, and H. A. Stone, Phys. Rev. Lett. **86**, 4704 (2001).

17 F. J. Almgren and J. E. Taylor, Sci. Am. **235**, 82 (1976).

18 J. A. Marquee and J. Ross, J. Chem. Phys. **79**, 373 (1983).

19 W. W. Mullins, J. Appl. Phys. **59**, 1341 (1986).

20 S. P. Marsh and M. E. Glicksman, Acta Mater. **44**, 3761 (1996).

21 I. M. Lifshitz and V. V. Slyozov, J. Phys. Chem. Solids **19**, 35 (1961).

22 C. Wagner, Z. Elektrochem. **65**, 581 (1961).

23 J. von Neumann (and following Reply by C. S. Smith), in *Metal Interfaces* (American Society for Metals, Cleveland, 1952), p. 108.

24 N. Rivier, Phil. Mag. B **47**, 91 (1983).

25 J. A. Glazier, Phys. Rev. Lett. **70**, 2170 (1993).

26 C. Sire, Phys. Rev. Lett. **72**, 420 (1994).

27 C. Monnereau, N. Pittet, and D. Weaire, Europhys. Lett. **52**, 361 (2000).

28 C. Monnereau and M. Vignes-Adler, Phys. Rev. Lett. **80**, 5228 (1998).

29 C. Monnereau, M. Vignes-Adler, and N. Pittet, Phil. Mag. B **79**, 1213 (1999).

30 C. Monnereau and M. Vignes-Adler, J. Colloid Interface Sci. **202**, 45 (1998).

31 K. Brakke, Exper. Math. **1**, 141 (1992).

32 http://www.susqu.edu/facstaff/b/brakke

33 A. M. Kraynik, D. A. Reinelt, and F. van Swol, in D. M. Binding et al. (Eds.), *Proceedings of the XIIIth International Congress on Rheology, Cambridge, UK*, pp. 1–43 (2000).

34 S. Hilgenfeldt, A. M. Kraynik, S. A. Koehler, and H. A. Stone, Phys. Rev. Lett. **86**, 2685 (2001).

35 H. Minkowski, Math. Ann. **57**, 447 (1903).

36 M. G. Kendall and P. A. P. Moran, *Geometrical probability* (Griffin, London, 1963).

37 N. Rivier, J. Phys. (Paris), Colloque C9 **43**, 91 (1982).

38 E. Matzke, Am. J. Bot. **33**, 58 (1946).

39 H. Flyvbjerg, Phys. Rev. E **47**, 4037 (1993).

40 M. F. Miri and N. Rivier, Europhys. Lett. **54**, 112 (2001).

41 D. Weaire and R. Phelan, Nature **367**, 123 (1994).

42 D. Weaire, N. Pittet, S. Hutzler, and D. Pardal, Phys. Rev. Lett. **71**, 2670 (1993).